



**HAL**  
open science

## In vitro compressive properties of skeletal muscles and inverse finite element analysis: comparison of human versus animals

Fuhao Mo, Zhefen Zheng, Haotian Zhang, Guibing Li, Zurong Yang, Deyi Sun

### ► To cite this version:

Fuhao Mo, Zhefen Zheng, Haotian Zhang, Guibing Li, Zurong Yang, et al.. In vitro compressive properties of skeletal muscles and inverse finite element analysis: comparison of human versus animals. Journal of Biomechanics, 2020, 109, pp.109916. 10.1016/j.jbiomech.2020.109916 . hal-03230539

**HAL Id: hal-03230539**

**<https://amu.hal.science/hal-03230539>**

Submitted on 20 May 2021

**HAL** is a multi-disciplinary open access archive for the deposit and dissemination of scientific research documents, whether they are published or not. The documents may come from teaching and research institutions in France or abroad, or from public or private research centers.

L'archive ouverte pluridisciplinaire **HAL**, est destinée au dépôt et à la diffusion de documents scientifiques de niveau recherche, publiés ou non, émanant des établissements d'enseignement et de recherche français ou étrangers, des laboratoires publics ou privés.



Distributed under a Creative Commons Attribution - NonCommercial - NoDerivatives 4.0 International License

# In vitro compressive properties of skeletal muscles and inverse finite element analysis: comparison of human versus animals

Fuhao MO <sup>1,3</sup>, Zhefen ZHENG <sup>1</sup>, Haotian ZHANG <sup>1</sup>, Guibing LI <sup>4</sup>, Zurong YANG <sup>5</sup>,  
Deyi Sun <sup>2\*</sup>

<sup>1</sup> State Key Laboratory of Advanced Design and Manufacture for Vehicle Body, Hunan University,  
Changsha, Hunan, 410082, China

<sup>2</sup> Department of Orthopedics, The Second Xiangya Hospital of Central South University, 139  
Renmin Road, Changsha, Hunan, 410011, China

<sup>3</sup> Aix-Marseille University, IFSTTAR, LBA UMRT24, Marseille, France

<sup>4</sup> School of Mechanical Engineering, Hunan University of Science and Technology, Xiangtan  
411201, China

<sup>5</sup> Department of Ultrasound, The Second Xiangya Hospital, Central South University, 139 Renmin  
Road, Changsha, Hunan 410011, China

1 **Abstract:** Virtual finite element human body models have been widely used in  
2 biomedical engineering, traffic safety injury analysis, etc. Soft tissue modeling like  
3 skeletal muscle accounts for a large portion of a human body model establishment, and  
4 its modeling method is not enough explored. The present study aims to investigate the  
5 compressive properties of skeletal muscles due to different species, loading rates and  
6 fiber orientations, in order to obtain **available** parameters of specific material laws as  
7 references for building or improving the human body model concerning both modeling  
8 accuracy and computational cost. **A series of compressive experiments of skeletal**  
9 **muscles were implemented for human gastrocnemius muscle, bovine and porcine hind**  
10 **leg muscle. To avoid long-time preservation effects, all experimental tests were carried**

11 out in 24 hours after that the samples were harvested. Considering computational cost  
12 and generally used in the previous human body models, one-order hyperelastic Ogden  
13 model and three-term simplified viscoelastic quasi-linear viscoelastic (QLV) were  
14 selected for numerical analysis. Inverse finite element analysis was employed to obtain  
15 corresponding material parameters. With good fitting records, the simulation results  
16 presented available material parameters for human body model establishment, and also  
17 indicated significant differences of muscle compressive properties due to species,  
18 loading rates and fiber orientations. When considering one-order Ogden law, it is  
19 worthy of noting that the inversed material parameters of the porcine muscles are  
20 similar to those of the human gastrocnemius regardless of fiber orientations. In  
21 conclusion, the obtained material parameters in the present study can be references for  
22 global human body and body segment modeling.

23 **Keywords:** Skeletal muscle, Human gastrocnemius, Inverse analysis, Finite element  
24 simulation, Parameter identification

25

## 26 **1. Introduction**

27 Finite element (FE) Human body models (HBMs) are widely used for biomechanical  
28 analysis in biomedical engineering, transport safety, sport science, and other human  
29 involved activities (Florio, 2018; Halloran, et al., 2010; Hedenstierna, et al., 2008;  
30 Lenhart, et al., 2015). Skeletal muscle accounts for about 40% of the body mass,  
31 therefore an understanding of its mechanical properties is important for virtual human  
32 body modeling and related biomechanical application (Chomentowski et al., 2011,  
33 Takaza, et al., 2013). Muscle tissues can be roughly characterized to be highly non-  
34 linear, viscoelastic, anisotropic and strain rate dependency like most biological tissues,  
35 while their properties can also vary significantly due to diversity of species. Thus, the  
36 experimental test and numerical modeling of muscle tissues are challenging works.

37

38 Skeletal muscle is composed of about 70-80% water, 3% fat and 10% collagen (Vignos  
39 and Lefkowitz, 1959). As it is very soft, most of the previous studies often tested it in  
40 compression setups. Partly due to experimental condition limitation, many previous  
41 studies primarily investigated mechanical behaviors of skeletal muscles in compression  
42 with different animal species, and obtained corresponding parameters with inverse  
43 analysis. For example, several previous studies (McElhaney, 1966; Van Loocke et al.,  
44 2006, 2008; Sligtenhorst and Cronin, 2006; Song et al., 2007; Chawla et al., 2009)  
45 investigated high strain rate effects of compression loading on skeletal muscles till  
46 3700/s, while other studies presented experimental results with relatively lower strain  
47 rates till 0.001/s (Sacks, 2000; Sligtenhorst et al., 2006; Song et al., 2007; Xu et al.,  
48 2011). With regard to fiber orientations, continuous researches were implemented with  
49 different animal muscles primarily considering the fiber orientations of 0°, 45° and 90°  
50 (Bosboom et al., 2001 a, b; Van Loocke et al., 2006; Böl et al., 2012; Mohammadkhan  
51 et al., 2016). Although the uniform macro feature of experimental curves can be noted  
52 for different animal muscles, the mechanical properties in detail during compression  
53 change a lot due to the species as well as experimental conditions. Thus, the limitations

54 of these animal muscle experiments for FE human body modeling **have** always existed.

55

56 To our knowledge, previous researchers on human skeletal muscle properties under  
57 compression loading were not enough and often limited to cadaver specimens with  
58 long-time **preservation**. Vannah et al. (1996) conducted quasi-static compression  
59 experiments of human muscles to provide design data for lower limb prostheses and  
60 other soft tissue supporting devices. Dhaliwal et al. (2002) conducted low energy  
61 impact tests on human cadaver muscles and obtained corresponding dynamic  
62 compressive mechanical properties. These previous studies primarily used the samples  
63 harvested from cadavers without indicating details of preservation conditions, like  
64 **preservation** time. However, the previous investigations have indicated that long term  
65 formalin preservation can significantly change mechanical properties of biological  
66 tissues, even for bone tissues (Kikugawa et al., 2004; Ohman et al., 2008; Zhang et al.,  
67 2019). Hence, we believe that implementing the experiments with short time  
68 **preservation** samples should be more **available** for soft tissues like skeletal muscle.

69

70 Hence, the objective of the present study was to investigate the compressive properties  
71 of human skeletal muscles with short term **preservation** less than 24 hours and compare  
72 them with those of other animals, in order to provide **available** modeling parameters for  
73 FE human modeling or related biomechanical application. In addition, many virtual FE  
74 human body or body segment models with skeletal muscle modeling **were** developed  
75 in the previous studies for various considerations, where the Ogden or QLV laws were  
76 usually used for these complicated model establishment (Mo et al., 2019). Here, we  
77 believe that in a FE human body modeling both accuracy and calculating efficiency  
78 should be considered for engineering application. Thus, two generally used material  
79 types for the global human body or segment models were selected to obtain specific  
80 material parameters by inverse finite element analysis in order to use them in **existing**  
81 or future FE human body models.

## 82 2. Materials and methods

### 83 2.1 Sample preparation and experimental procedure

84 All experiments were approved by the ethics committee of the Second Xiangya  
85 Hospital of Central South University (NO. 2012-S231) and the informed consent was  
86 obtained from the patients participating in the study. Cubic muscle samples with a  
87 characteristic edge length of 10 mm were obtained from human gastrocnemius muscle  
88 as well as bovine and porcine hind legs. Summary of sample sizes is listed in Table 1.  
89 The bovine samples were harvested from the hindquarter of a large Yorkshire, and the  
90 porcine samples were harvested from the hindquarter of a Chinese yellow cattle. The  
91 human gastrocnemius muscle was obtained from two amputee donators (age  $69\pm 3$  years  
92 old) without any leg muscle disorders or diseases. The tissues were fixed using formalin  
93 to prevent tissue dissolution for no more than 24 hours before the experiments.

94

95 Before the experiment, the skin, fat and fascia were firstly removed from the muscle  
96 tissues to obtain standard cubic testing specimens. All operations were carried out by a  
97 surgeon through a scalpel and an assistive block with ruler to control the size.  
98 Subsequent compressive experiments were performed using different loading rates and  
99 along different fiber orientations ( $0^\circ$ ,  $45^\circ$  and  $90^\circ$ ) as shown in Fig. 1. The MTS E45  
100 electronic universal testing machine was used to compress the specimens up to 50%  
101 strain at rates of 0.05%/s, 0.5%/s and 5%/s. The measurement range of the selected  
102 force sensor is 30kN with a resolution of 0.001N. As pre-compression may lead to  
103 unpredictable permanent tissue deformation, each specimen was tested once and no  
104 precondition was applied to the specimen. At least three successful specimen tests were  
105 achieved at each testing condition. A total of successful 99 compression experiments  
106 were conducted at different loading rates and fiber directions.

107 **Fig.1. Schematic of compression experiments with different loading rates and fiber**  
108 **directions**

**Table 1. Sample size and average specimen dimensions at different fiber orientations**

Specimen	Fiber direction	Average height $\pm$ std (mm)	Average width $\pm$ std (mm)	Average thickness $\pm$ std (mm)	Sample size (N)
Bovine	0°	10.5±0.6	10.7±0.5	10.5±0.6	12
	45°	10.8±1.2	11.1±1.2	10.6±0.6	12
	90°	10.9±0.9	10.8±0.7	10.8±0.7	12
Porcine	0°	11.3±0.9	10.8±0.8	10.9±0.9	12
	45°	11.1±1.4	10.5±1.1	10.5±0.5	12
	90°	11.7±0.8	11.3±0.9	10.8±0.7	12
Human	0°	10.0±1.0	10.7±0.5	10.3±0.5	9
	45°	9.9±0.9	10.4±0.8	10.1±0.7	9
	90°	12.0±2.1	10.6±1.9	10.3±0.9	9

## 110 2.2 Mathematical modeling

111 Following the previous studies (Comley et al. 2012, Takaza et al. 2013, Mo et al, 2018,  
 112 2019a, b), one-order Ogden hyperelastic material law and three-terms quasi-linear  
 113 viscoelastic (QLV) material law were usually selected for modeling passive behavior  
 114 of muscle tissues **in human body models**. The Ogden hyperelastic material law is  
 115 expressed as follows,

$$116 \quad W = \sum_{i=1}^n \frac{\mu_i}{\alpha_i} (\lambda_1^{\alpha_i} + \lambda_2^{\alpha_i} + \lambda_3^{\alpha_i} - 3) + K(J - 1 - \ln J) \quad (1)$$

117 Where  $W$  is the strain energy of the model;  $\mu$  is the initial shear modulus,  $\alpha$  is the  
 118 deviatoric exponent,  $\lambda_i$  is the deviatoric principal stretches in three directions: x, y and  
 119 z;  $J$  represents the bulk modulus. The skeletal muscle was considered incompressible,  
 120 thus,  $J$  equaled to 1. Therefore, the simple one-order Ogden law is expressed as follows,

$$121 \quad W = \frac{2\mu}{\alpha^2} (\lambda_1^\alpha + \lambda_2^\alpha + \lambda_3^\alpha - 3) \quad (2)$$

122 The viscoelastic QLV law is expressed as equation (3) and (4),

$$123 \quad \sigma(t) = \int_0^t G(t - \tau) \frac{\partial \sigma^e(\lambda)}{\partial \lambda} \cdot \frac{\partial \lambda}{\partial \tau} d\tau \quad (3)$$

124 Where  $\partial \sigma^e(\lambda)/\partial \lambda$  is the instantaneous elastic response,  $\partial \lambda/\partial \tau$  is the stretch history;  
125  $G(t - \tau)$  is the relaxation function.

126 Based on the QLV law, we used a simplified model focusing on instantaneous elastic  
127 response in compression. And three terms of model coefficients were adopted. The  
128 equation is expressed as follows,

$$129 \quad \sigma_\varepsilon(\varepsilon) = C_1 \varepsilon^1 + C_2 \varepsilon^2 + C_3 \varepsilon^3 \quad (4)$$

130 Where  $C_1$ ,  $C_2$  and  $C_3$  are the coefficients of instantaneous elastic responses;  $\varepsilon^1$ ,  $\varepsilon^2$   
131 and  $\varepsilon^3$  are the principal strains in three directions.

### 132 2.3 Inverse analysis

133 Inverse analysis has been applied for defining material parameters of soft tissues (Ahn,  
134 et al., 2010; Chawla, et al., 2009; Böl, et al., 2012; Nava, et al., 2008; Samur, et al.,  
135 2005, 2007). The purpose of the inverse analysis was to minimize the error between the  
136 experimental results and simulation responses by using an optimization algorithm to  
137 identify optimal material parameters (Böl, et al., 2012). The agreement between  
138 experimental results and simulation results were evaluated by the objective function as  
139 follows,

$$140 \quad f(x) = \sqrt{\frac{\sum_i^n (F_i^{exp} - F_i^{FEM})^2}{n}} \quad (5)$$

141 Where  $F_i^{exp}$  is the experimental force value,  $F_i^{FEM}$  is the responsive force of finite  
142 element simulation, and  $n$  is the number of data points. The process of inverse analysis  
143 for material parameter identification is described in the following section.

## 144 2.4 Identification of material parameters

145 To identify material parameters of the tested skeletal muscles, a method combining  
146 inverse solve and finite element optimization of material parameters were employed, as  
147 shown in Fig. 2. The errors between the simulation and experimental results are  
148 calculated by equation (5). A custom python program using a least-squares algorithm  
149 was firstly used to fit experimental results to acquire initial parameters of the  
150 corresponding laws. Then, their values were optimized and finally determined by  
151 inversed finite element analysis. Adaptive response surface method (ARSM) was  
152 adopted in the FE simulations to minimize the error and obtain optimal parameters until  
153 calculation convergence referring to the previous study (Wang et al.,2007), which is a  
154 direct optimization method based on response surface. The basic idea of ARSM method  
155 is to construct a response surface with fewer sample points first and determine the  
156 optimization direction. During the optimization process, new design points are obtained  
157 along the gradient direction of the response surface, and introduced into the design  
158 space so that the response surface model can be gradually updated to improve  
159 optimization efficiency and fitting accuracy. By optimizing and updating the response  
160 surface, the optimal solution can be continuously approached to the real optimal  
161 solution.

### 162 Fig.2. Schematic illustration of material parameter identification

163 The FE simulations were implemented with Ls-Dyna codes. The specimen was meshed  
164 with hexahedral solid elements of the size 1 mm by Hypermesh software. Element  
165 quality was checked to avoid distorted elements and to satisfy the minimum time step  
166 criteria. The time step was set as 1.0e-5. Surface to surface contacts were defined  
167 between the platens and the specimen, and a self-contact of the specimen was defined  
168 to avoid solid collapse during large deformation. The lower platen was constrained with  
169 no freedom in all directions, while the upper platen can freely translate along the  
170 compression direction. The friction coefficient between the platen and specimen was  
171 set as 0.3 according to the previous study (Wu, et al., 2004).

172 **3. Results**

173 **3.1 Experimental results**

174 Characteristic compressive stress-strain responses are classified based on tissue fiber  
175 orientations, compression strain rates and species (Fig. 3-Fig. 5). The bovine and  
176 porcine muscle properties are illustrated in Fig. 3 and Fig. 4, respectively. Compressive  
177 responses of the human gastrocnemius muscles are shown in Fig. 5. As general soft  
178 biological tissues, the experimental data of the muscle tissues scatter on a large scale in  
179 the present study. When comparing compressive responses of different species as  
180 shown in Fig. 6, the substantial difference can be noted due to species, fiber orientations  
181 and strain rates. The compressive properties of the porcine muscles seem to be closer  
182 to the human gastrocnemius muscles than those of the bovine muscles.

183

184 In most testing conditions except for 90° bovine muscle, potential strain effects are  
185 noted in the testing range from 0.05% to 5% for all species and fiber orientations, while  
186 the Cauchy stress value inclines significantly with the increasing strain rate at 50%  
187 strain as shown in Fig. 6 ( $p < 0.005$ ). With the increase of the strain rate, the scattering  
188 range of the compressive curves in most of testing conditions tends to enlarge. The  
189 stiffest tissue response was obtained when the muscle fibers were oriented in  
190 perpendicular to the loading direction (90° fiber orientation), followed by a fiber  
191 orientation of 45°. Fiber orientation of 0° in parallel with the loading direction yielded  
192 the softest response.

193 (a) 0° (b) 45° (c) 90°

194 **Fig.3. Compressive stress-stretch responses of the bovine muscles at various rates and fiber**  
195 **orientations**

196 (a) 0° (b) 45° (c) 90°

197 **Fig.4. Compressive stress-stretch responses of the porcine muscles at various rates and fiber**

orientations

(a) 0° (b) 45° (c) 90°

**Fig.5. Compressive stress-stretch responses of the human gastrocnemius muscles at various rates and fiber orientations**

**Fig.6. Comparison of compressive responses of different species under a strain level of 50%**

### 3.2 Identification of material parameters

We used the averaged experimental curves of different fiber orientations and different species as the objective curves for the optimization of material parameters. Through the above-mentioned method, the typical fitting results of numerical simulations to experimental results considering the human skeletal muscles of three fiber orientations are shown in Fig. 7. All simulation results are in good agreement with the experimental responses.

Inversed material parameters of different muscle tissues using one-order Ogden law were illustrated in Table 2. The corresponding material parameters of three-terms **simplified** QLV law were listed in Table 3. For both material laws, the obtained material parameters for different species and fiber orientations present some differences. Although significant differences ( $p < 0.05$ ) of material parameters existed between the porcine and human muscles considering different fiber orientations, the inversed material parameters **of the averaged curves of all three fiber orientations show similar values for both human ( $\mu=3.43$  kPa,  $\alpha=8.74$ ) and porcine ( $\mu=3.63$  kPa,  $\alpha=8.74$ ) muscles** concerning one-order Ogden law.

(a) 0° (b) 45° (c) 90°

**Fig.7. Typical fitting results of the finite element simulations to the experimental results of the human skeletal muscles.**

**Table 2 Optimized muscle material parameters of one-order Ogden law**

Species	Fiber orientation	Material parameters	R <sup>2</sup> (FE)	RMSE
Bovine	0°	$\mu=0.26$ kPa $\alpha=14.00$	0.994	1.21
	45°	$\mu=0.65$ kPa $\alpha=13.83$	0.998	1.67
	90°	$\mu=2.00$ kPa $\alpha=10.11$	0.997	8.91
	Average	$\mu=1.18$ kPa $\alpha=11.97$	0.998	2.12
Porcine	0°	$\mu=0.54$ kPa $\alpha=14.00$	0.983	11.07
	45°	$\mu=3.80$ kPa $\alpha=9.00$	0.969	115.50
	90°	$\mu=3.96$ kPa $\alpha=8.92$	0.994	23.08
	Average	$\mu=3.63$ kPa $\alpha=8.74$	0.983	40.59
Human	0°	$\mu=2.24$ kPa $\alpha=8.97$	0.989	15.72
	45°	$\mu=3.77$ kPa $\alpha=9.00$	0.982	63.88
	90°	$\mu=5.07$ kPa $\alpha=9.14$	0.994	43.79
	Average	$\mu=3.43$ kPa $\alpha=8.74$	0.934	173.33

**Table 3 Optimized muscle material parameters of three-terms QLV law**

Species	Fiber orientation	Material parameters	R <sup>2</sup> (FE)	RMSE
Bovine	0°	C1=88.61 C2=-772.05 C3=1716.00	0.937	18.74
	45°	C1=169.70 C2=-1500.86 C3=3607.17	0.957	45.73
	90°	C1= 132.00 C2= -1140.00 C3=3320.00	0.960	79.09
	Average	C1= 122.18 C2= -1065.46 C3=2808.00	0.978	26.77
Porcine	0°	C1=90.00 C2= -1088.22 C3=2849.00	0.977	22.26
	45°	C1=99.00 C2= -994.16 C3=3366.99	0.992	22.51
	90°	C1=189.00 C2= -1477.87 C3=4488.00	0.991	36.25
	Average	C1= 132.00 C2=-990.00 C3=2981.00	0.982	40.32
Human	0°	C1= 115.36 C2= -965.06 C3=2758.01	0.967	42.45

45°	C1= 165.00 C2= -1160.00 C3=3310.00	0.964	76.57
90°	C1=436.05 C2= -3124.03 C3=7616.21	0.941	367.21
average	C1=253.00 C2=-1810.00 C3=4590.00	0.945	152.51

---

228 Notes: RMSE represents Root Mean Squared Error.

## 229 4. Discussion

230 Although some previous studies have investigated skeletal muscle properties in  
231 different loading types using different animal specimens (Mohammadkhah et al.,2016,  
232 Nie et al.,2011, Simms et al.,2012, Takaza et al.,2013a), the experimental results of  
233 human skeletal muscles especially the data with short preservation time in formalin or  
234 in status were rare. In the present study, we aim to provide material properties for human  
235 body modeling, especially in the application of comfort and impact analysis during  
236 seating and car crash. In these two loading conditions, human body muscles generally  
237 experience a compression loading. In addition, when we compared the published  
238 muscle properties of different animals (Song et al., 2007, Dhaliwal et al., 200,  
239 Mohammadkhah et al.,2016, Van Sligtenhorst et al.,2006, Takaza et al.,2014),  
240 substantial differences of mechanical behaviors in compression can be noted. Hence,  
241 the first purpose of this study was to investigate compressive behaviors of human  
242 skeletal muscle without long formalin storing time, then obtain their material  
243 parameters of generally used and computationally efficient material laws for the  
244 improvement or establishment of human body models. By the way, the dominant fiber  
245 directions can be different considering anatomic structures of different muscles. Muscle  
246 compressive properties from three representative fiber directions were measured and  
247 analyzed. Compressive properties of muscle tissues in other fiber directions should be  
248 located between them. In the establishment of a related human body model, we  
249 recommended either establishing or employing an anisotropic constitutive material law  
250 in the model, or optimizing the corresponding muscle parameters of the available  
251 isotropic laws considering fiber distribution and boundary loading conditions.

252

253 The Cauchy stress-strain relationship presented in this study provided a reference for  
254 investigating mechanical behaviors of human skeletal muscles. The results showed that  
255 the Cauchy stress during compression increased with the increasing strain rate, which  
256 was similar to the previous researches (Chawla, et al., 2009; Sligtenhorst, et al., 2006;  
257 Song, et al., 2007; Van Loocke, et al., 2006; Van Loocke, et al., 2008). The Cauchy  
258 stress of 50% compression strain at the compression loading rate of 5%/s was about 3  
259 times larger than that at the compression rate of 0.05%/s, which was qualitatively  
260 similar to the results at other strain rates (Van Loocke, et al., 2006; Van Loocke, et al.,  
261 2008). The cross-fiber orientation mechanical response was found to be stiffer than  
262 other fiber orientations, which was similar to the findings of the previous researches  
263 with different loading strain rates (Song, et al., 2007; Böl, et al., 2012).

264

265 As the inversed material parameters shown in Table 2, the optimized shear modulus  $\mu$   
266 of 5.07 kPa for human gastrocnemius was close to in vivo experimental results using  
267 supersonic shear wave elastography (SWE) of Mäissetti et al. (2012) study or the results  
268 of our verifying measurements. This can indicate the reliability of our results, and that  
269 the obtained tissue properties are close to in vivo muscle tissue properties. In addition,  
270 the average inversed material parameters of one-order Ogden law regardless of fiber  
271 orientations for the porcine and human muscles are similar. But those of the bovine  
272 muscle **are largely** different with them. To some extent, it could indicate that using  
273 porcine muscle for experimental tests could provide more useful information for human  
274 muscle tissue modeling if the human tissue experiment is limited. But it can be also  
275 influenced by native species' difference. To extend experimental possibility, we believe  
276 that it is important to find proper alternative animal tissues with similar mechanical  
277 properties to human tissues for experimental researches.

278

279 The present study selected one-order Ogden law for skeletal muscle modeling, as it is  
280 a simple and reasonable solution for soft tissue modeling. Especially concerning its

281 application in a global biomechanical model, the high computational efficiency was  
282 extremely appreciated in our previous foot model and lower limb modeling (Mo et al.,  
283 2018, 2019). We compared the computational cost of one-order Ogden law and three-  
284 terms simplified QLV law in the present compression modeling using Ls-Dyna solver.  
285 With 8-core Xeon® CPU, the calculation time for a simple compression simulation is  
286 23 min and 27mins, respectively. The one-order Ogden law has some advantages in  
287 saving computational cost as well as controlling the stability of a global human body  
288 model for loading conditions without large concerns on viscoelasticity. Considering a  
289 global human body or large body segment modeling, we believe the balance of  
290 modeling accuracy and computational cost should be achieved properly with regard to  
291 research objectives.

292

293 The present study combined experimental tests and inverse analysis method to  
294 investigate the effects of loading rate, fiber orientation and species differences on  
295 compressive behaviors of skeletal muscles. A large number of experiments and  
296 numerical simulations were implemented, and **available** material parameters were  
297 obtained for human body modeling reference. There are still several limitations. First,  
298 the limited sample size for each testing condition may partly limit part of the robustness  
299 of our results. As limited pure muscle tissues can be obtained after removing other fiber  
300 tissues in one donator, we had to harvest samples from two amputees not as we can  
301 obtain all muscle samples from one animal. But if we enlarge our sample size, the  
302 effects of individuals' difference would be also extended. Second, we use an ideal and  
303 standard geometry for inverse finite element analysis to obtain muscle material  
304 parameters. As indicated by the previous study (Böl et al, 2012), to further precisely  
305 define the muscle parameters, an inverse finite element method with detailed geometry  
306 definition could be more powerful. Additionally, we also believe that using **short-time**  
307 **preservation** tissues for experiments or adopting in-vivo measuring methods like the  
308 SWE method for obtaining or evaluating material parameters can be further  
309 investigated for virtual FE human model establishment.

## 310 **5. Conclusion**

311 Inspired by the objective of human body modeling, the present study investigated the  
312 compressive properties of skeletal muscles with different species, loading rates and  
313 fiber orientations. Two commonly used material laws of Ogden and QLV constitutive  
314 models were selected and **simplified** for numerical analysis in the consideration of  
315 computational efficiency and modeling accuracy. Optimized material parameters were  
316 well obtained through inverse analysis based on custom-made codes and optimal finite  
317 element simulations, which can be **available** references for human body modeling. The  
318 experimental results show **substantial** differences between species, loading rates and  
319 fiber orientations. Referring to the material parameters of one-order Ogden law, similar  
320 values between the porcine muscles and the human gastrocnemius were found  
321 regardless of fiber orientations. The inversed shear modulus was further verified by in  
322 vivo SWE measurement, thus it also indicated that the present parameters can reflect  
323 the properties of in vivo human gastrocnemius muscle. Coupling experimental and  
324 simulation investigations on different human muscles could be extended in the future  
325 to further evaluate the present method and findings.

## 326 **Conflict of interest statement**

327 The authors assert that there are no conflicts of interest of any type.

## 328 **Acknowledgments**

329 This study was supported by the National Key Research and Development Program of  
330 China (2018YFC1105800), National Natural Science Foundation of China (Grant No.  
331 51875187, 51621004), and Hunan Province Science and Technology Plan (Grant No.  
332 2019JJ40021). We also thank gratefully to Dr. Tang Liu's and Dr. Pengcheng Dou's  
333 help for experimental tests.

## Reference

1. Ahn, B., and J. Kim. 2010. Measurement and characterization of soft tissue behavior with surface deformation and force response under large deformations [J]. *Med. Image. Anal.* 14(2):138-148, 2010.
2. Böl, M., R. Kruse, A. E. Ehret, K. 2012. Leichsenring, and T. Siebert. Compressive properties of passive skeletal muscle-The impact of precise sample geometry on parameter identification in inverse finite element analysis [J]. *J. Biomech.* 45(15):2673-2679.
3. Bosboom, E. M. H., M. K. C. Hesselink, C. W. J. Oomens, C. V. C. Bouten, M. R. Drost, and F. P. T. Baaijens. 2001. Passive transverse mechanical properties of skeletal muscle under in vivo compression [J]. *J. Biomech.* 34(10):1365-1368.
4. Bosboom, E. M. H., J. A. M. Thomassen, C. W. J. Oomens, C. V. C. Bouten, and F. P. T. Baaijens. 2001. A numerical-experimental approach to determine the transverse mechanical properties of skeletal muscle [C], J. Middleton, M.L. Jones, N.G. Shrive(Eds.), *Computer Methods In Biomechanics And Biomedical Engineering*, 3, Gordon and Breach Sciences Publishers, Ne York, pp. 187-192.
5. Chawla, A., S. Mukherjee, and B. Karthikeyan. 2009. Characterization of human passive muscles for impact loads using genetic algorithm and inverse finite element methods [J]. *Biomech. Model. Mechan.* 8(1):67-76, 2009.
6. Chomentowski, P., P. M. Coen, Z. Radikova, B. H. Goodpaster, and F. G. S. Toledo. 2011. Skeletal Muscle Mitochondria in Insulin Resistance: Differences in Intermyoibrillar Versus Subsarcolemmal Subpopulations and Relationship to Metabolic Flexibility [J]. *J. Clin. Endocrinol. Metab.* 96(2):494-503.
7. Comley, K., and N. Fleck. 2012. The compressive response of porcine adipose tissue from low to high strain rate [J]. *Int. J. Impact. Eng.* 46:1-10.
8. Dhaliwal, T. S., P. Beillas, C. C. Chou, P. Prasad, K. H. Yang, and A. I. King. 2002.

Structural response of lower leg muscles in compression: a low impact energy study employing volunteers, cadavers and the hybrid III [J]. *Stapp. Car . Crash. J.* 46:229-243.

9. Florio, C. S. 2018. Effectiveness of various isometric exercises at improving bone strength in cortical regions prone to distal tibial stress fractures [J]. *Int. J. Numer. Method. Biomed. Eng.* 34(6): e2976.
10. Halloran, J. P., M. Ackermann, A. Erdemir, and A. J. van den Bogert. 2010. Concurrent musculoskeletal dynamics and finite element analysis predicts altered gait patterns to reduce foot tissue loading [J]. *J. Biomech.* 43(14):2810-2815.
11. Hedenstierna, S., P. Halldin, and K. Brolin. 2008. Evaluation of a combination of continuum and truss finite elements in a model of passive and active muscle tissue [J]. *Comput. Methods. Biomech. Biomed. Eng.* 11(6):627-639.
12. Kikugawa, H., and T. Asaka. 2004. Effect of long-term formalin preservation on bending properties and fracture toughness of bovine compact bone [J]. *Mater. Trans.* 45(10):3060-3064.
13. Lenhart, R. L., J. Kaiser, C. R. Smith, and D. G. Thelen. 2015. Prediction and Validation of Load-Dependent Behavior of the Tibiofemoral and Patellofemoral Joints During Movement [J]. *Ann. Biomed. Eng.* 43(11):2675-2685.
14. Maisetti, O., F. Hug, K. Bouillard, and A. Nordez. 2012. Characterization of passive elastic properties of the human medial gastrocnemius muscle belly using supersonic shear imaging [J]. *J. Biomech.* 45(6):978-984.
15. McElhaney, J. H. 1966. Dynamic response of bone and muscle tissue [J]. *J. Appl. Physiol.* 21(4):1231-1236.
16. Mo, F., F. Li, M. Behr, Z. Xiao, G. Zhang, and X. Du. 2018. A Lower Limb-Pelvis Finite Element Model with 3D Active Muscles [J]. *Ann. Biomed. Eng.* 46(1):86-96.
17. Mo, F., J. Li, M. Dan, T. Liu, and M. Behr. 2019. Implementation of controlling

- strategy in a biomechanical lower limb model with active muscles for coupling multibody dynamics and finite element analysis [J]. *J. Biomech.* 91:51-60.
18. Mo, F., J. Li, Z. Yang, S. Zhou, and M. Behr. 2019. In Vivo Measurement of Plantar Tissue Characteristics and Its Indication for Foot Modeling [J]. *Ann. Biomed. Eng.* 47: 2356-2371.
  19. Mohammadkhah, M., P. Murphy, and C. K. Simms. 2016. The in vitro passive elastic response of chicken pectoralis muscle to applied tensile and compressive deformation [J]. *J. Mech. Behav. Biomed. Mater.* 62:468-480.
  20. Nava, A., E. Mazza, M. Furrer, P. Villiger, and W. H. Reinhart. 2018. In vivo mechanical characterization of human liver [J]. *Med. Image. Anal.* 12(2):203-216.
  21. Nie, X., J.-I. Cheng, W. W. Chen, and T. Weerasooriya. 2011. Dynamic Tensile Response of Porcine Muscle [J]. *J. Appl. Mech.* Mar 2011, 78(2): 021009-14.
  22. Ohman, C., E. Dall'Ara, M. Baleani, S. V. S. Jan, and M. Viceconti. 2008. The effects of embalming using a 4% formalin solution on the compressive mechanical properties of human cortical bone [J]. *Clin. Biomech.* 23(10):1294-1298.
  23. Sacks, M. S. 2000. Biaxial mechanical evaluation of planar biological materials [J]. *J. Elast.* 61(1-3):199-246.
  24. Samur, E., M. Sedef, C. Basdogan, L. Avtan, and O. Duzgun. 2005. A robotic indenter for minimally invasive characterization of soft tissues [C], in *CARS 2005: Computer Assisted Radiology and Surgery*, edited by H. U. Lemke, K. Inamura, K. Doi, M. W. Vannier, and A. G. Farman, 713-718.
  25. Samur, E., M. Sedef, C. Basdogan, L. Avtan, and O. Duzgun. 2007. A robotic indenter for minimally invasive measurement and characterization of soft tissue response [J]. *Med. Image. Anal.* 11(4):361-373.
  26. Simms, K.C., Van Looke, M., Lyons, C.G., 2012. Skeletal muscle in compression:modelling approaches for the passive muscle bulk [J]. *Int. J.*

Multiscale. Com. 10 (2), 143 – 154.

27. Song, B., W. Chen, Y. Ge, and T. Weerasooriya. 2007. Dynamic and quasi-static compressive response of porcine muscle [J]. *J. Biomech.* 40(13):2999-3005.
28. Takaza, M., Cooney, G.M., Mcmanus, G., Stafford, P., Simms, C.K.,2014. Assessing the microstructural response to applied deformation in porcine passive skeletal muscle.[J]. *J. Mech. Behav. Biomed. Mater.* 40: 115-126.
29. Takaza, M., Moerman, K.M., Gindre, J., Lyons, G., Simms, C.K.,2013a. The anisotropic mechanical behaviour of passive skeletal muscle tissue subjected to large tensile strain.[J]. *J. Mech. Behav. Biomed. Mater.* 17: 209-220.
30. Takaza, M., K. M. Moerman, and C. K. Simms. 2013. Passive skeletal muscle response to impact loading: Experimental testing and inverse modelling [J]. *J. Mech. Behav. Biomed. Mater.* 27:214-225.
31. Van Loocke, M., C. G. Lyons, and C. K. Simms. 2006. A validated model of passive muscle in compression [J]. *J. Biomech.* 39(16):2999-3009.
32. Van Loocke, M., C. G. Lyons, and C. K. Simms. 2008. Viscoelastic properties of passive skeletal muscle in compression: Stress-relaxation behaviour and constitutive modelling [J]. *J. Biomech.* 41(7):1555-1566.
33. Van Sligtenhorst, C., D. S. Cronin, and G. W. Brodland. 2006. High strain rate compressive properties of bovine muscle tissue determined using a split Hopkinson bar apparatus [J]. *J. Biomech.* 39(10):1852-1858.
34. Vannah, W. M., and D. S. Childress. 1996. Indentor tests and finite element modeling of bulk muscular tissue in vivo [J]. *J. Rehabil. Res. Dev.* 33(3):239-252.
35. Vignos, P. J., Jr., and M. Lefkowitz. 1959. A biochemical study of certain skeletal muscle constituents in human progressive muscular dystrophy [J]. *J. Clin. Invest.* 38(6):873-881.
36. Wang, H., G. Li and Z. Zhong. 2008. Optimization of sheet metal forming processes

by adaptive response surface based on intelligent sampling method [J]. *J. Mater. Process. Tech.* 197(1-3), 77-88.

37. Wu, J. Z., R. G. Dong, and A. W. Schopper. 2004. Analysis of effects of friction on the deformation behavior of soft tissues in unconfined compression tests [J]. *J. Biomech.* 37(1):147-155.
38. Zhang, G., S. Wang, S. Xu, F. Guan, Z. Bai, and H. Mao. 2019. The Effect of Formalin Preservation Time and Temperature on the Material Properties of Bovine Femoral Cortical Bone Tissue [J]. *Ann. Biomed. Eng.* 47(4):937-952.

## Figure legends

Figure 1. Schematic of compression experiments with different loading rates and fiber directions.

Figure 2. Schematic illustration of material parameter identification.

Figure 3. Compressive stress-stretch responses of the bovine muscles at various rates and fiber orientations. (a)  $0^\circ$  (b)  $45^\circ$  (c)  $90^\circ$

Figure 4. Compressive stress-stretch responses of the porcine muscles at various rates and fiber orientations. (a)  $0^\circ$  (b)  $45^\circ$  (c)  $90^\circ$

Figure 5. Compressive stress-stretch responses of the human gastrocnemius muscles at various rates and fiber orientations. (a)  $0^\circ$  (b)  $45^\circ$  (c)  $90^\circ$

Figure 6. Comparison of compressive responses of different species under a strain level of 50%.

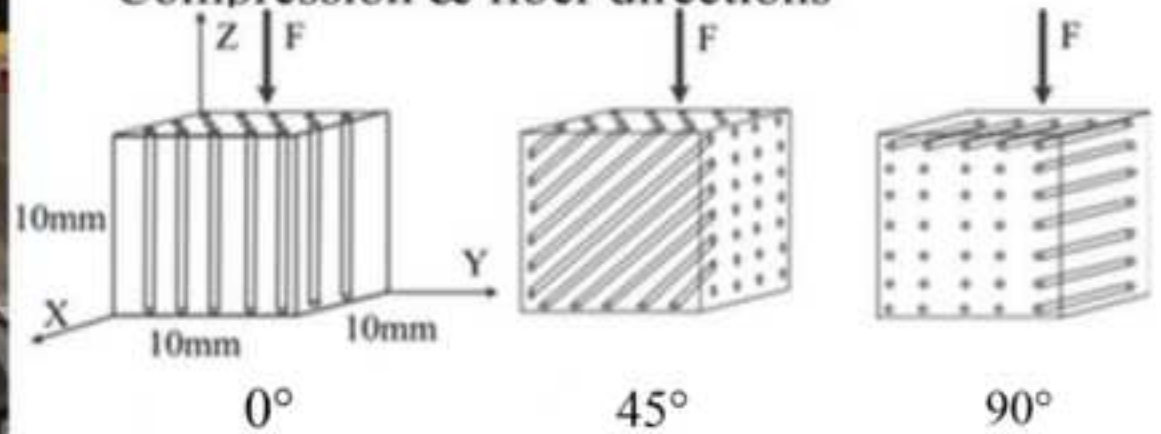
Figure 7. Typical fitting results of the finite element simulations to the experimental results of the human skeletal muscles. (a)  $0^\circ$  (b)  $45^\circ$  (c)  $90^\circ$



Specimen

Lower Platen

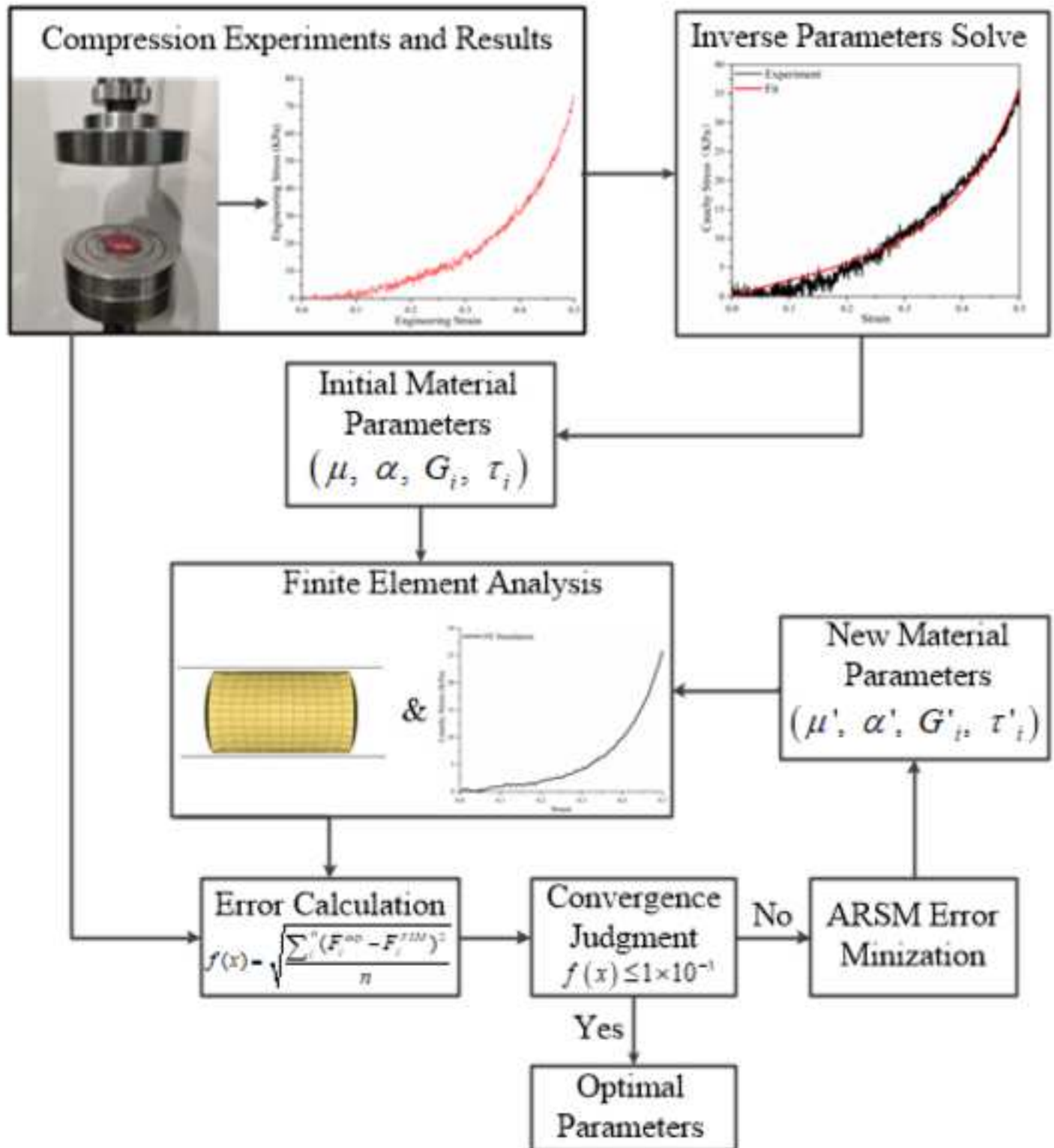
Compression & fiber directions

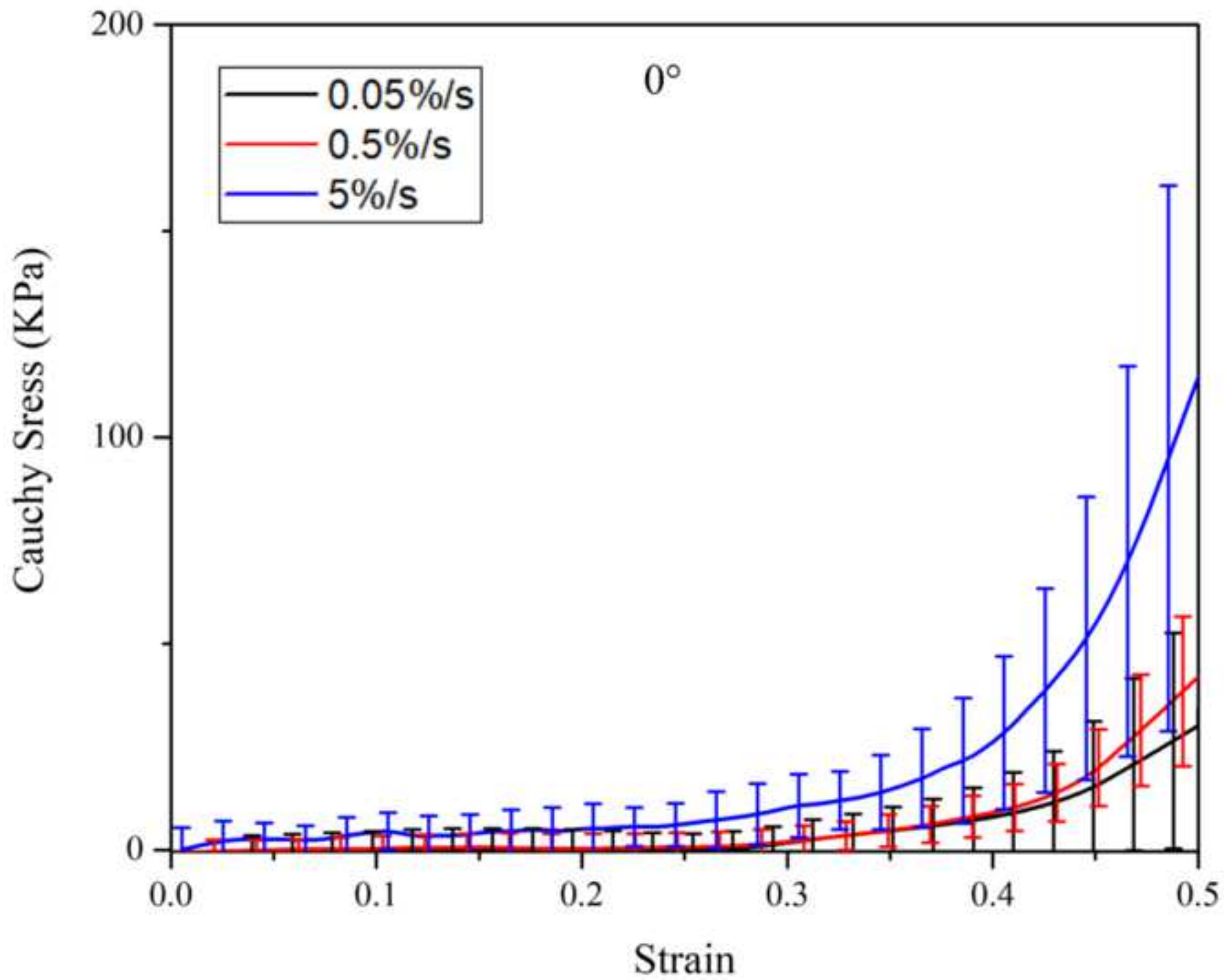


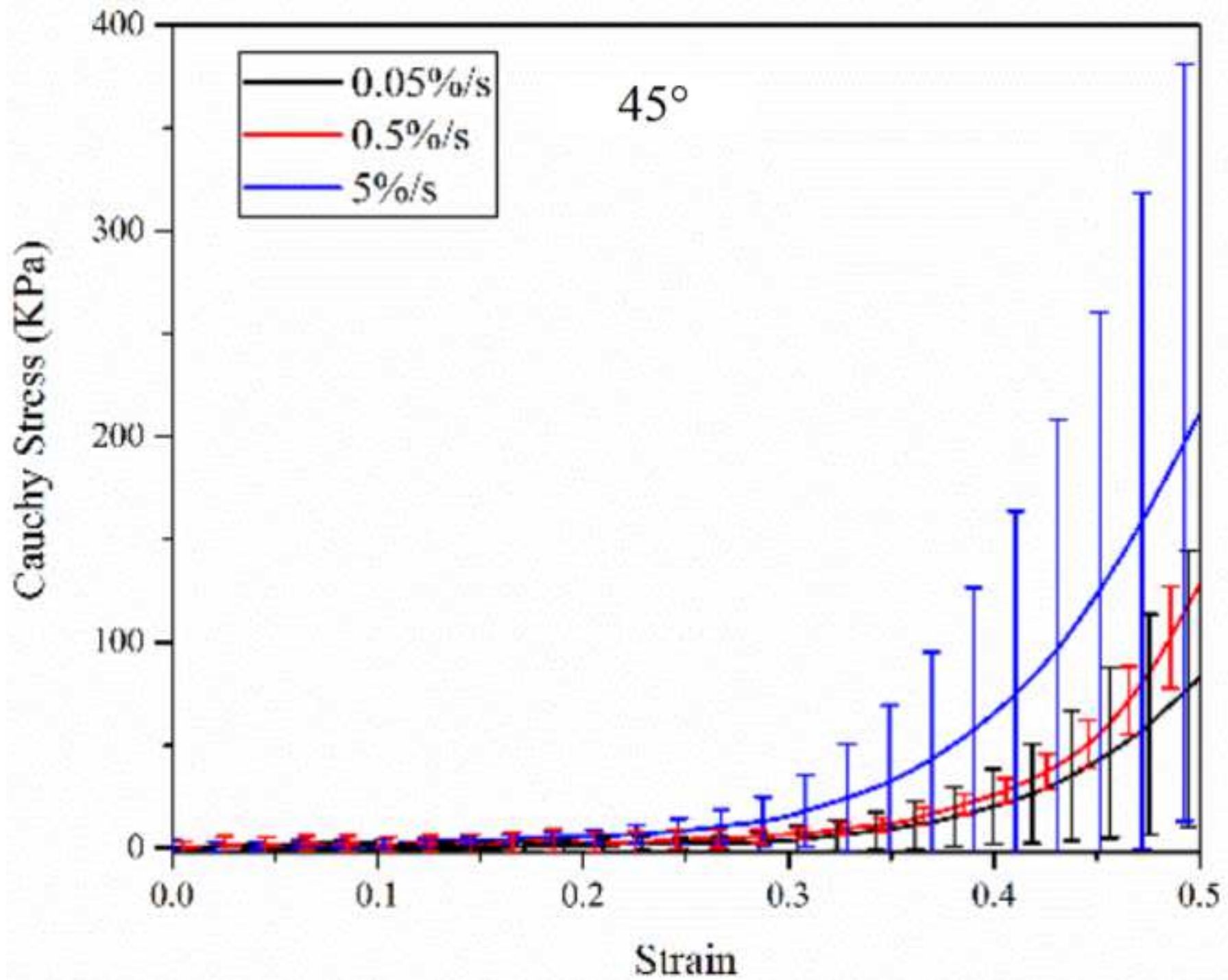
$0^\circ$

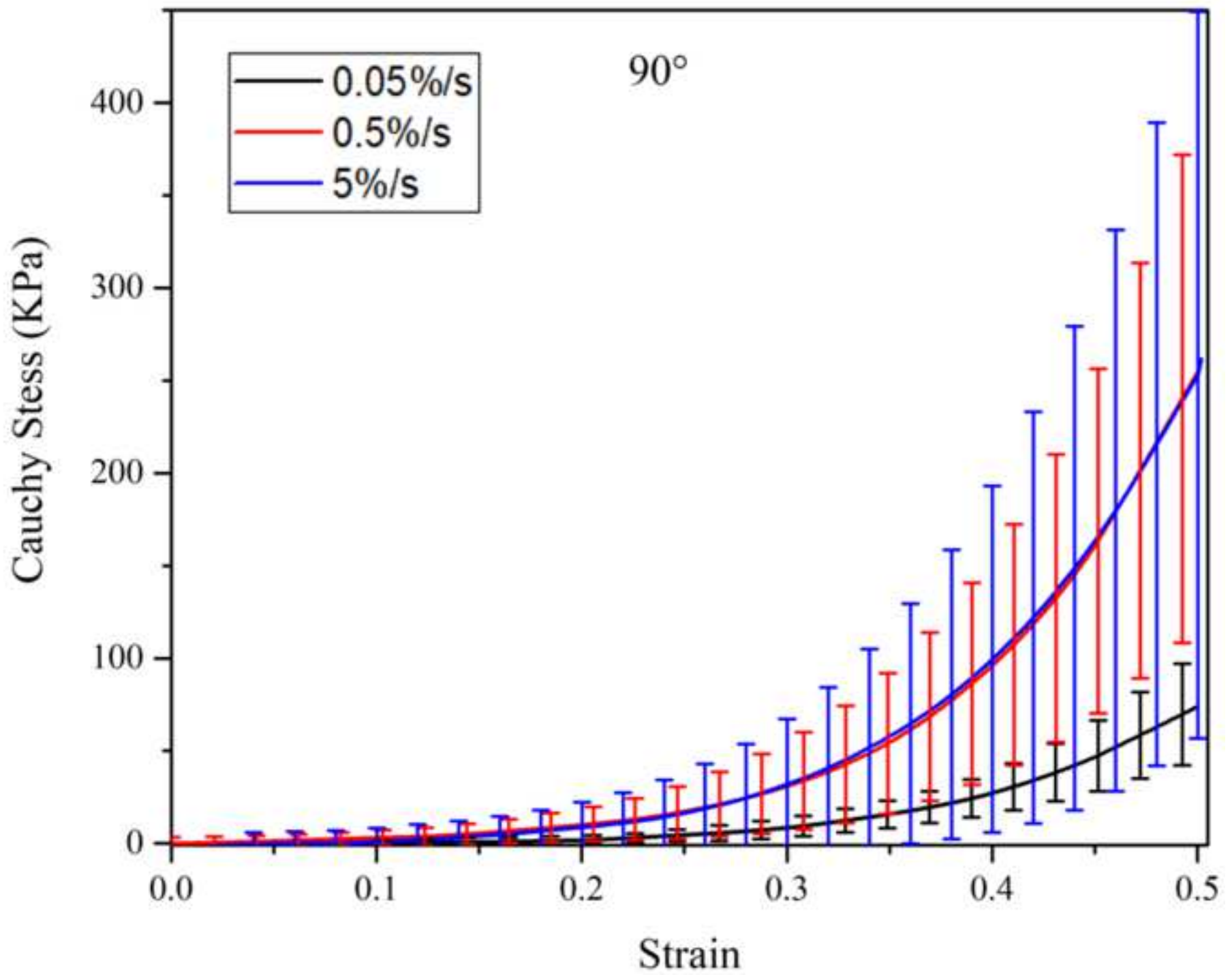
$45^\circ$

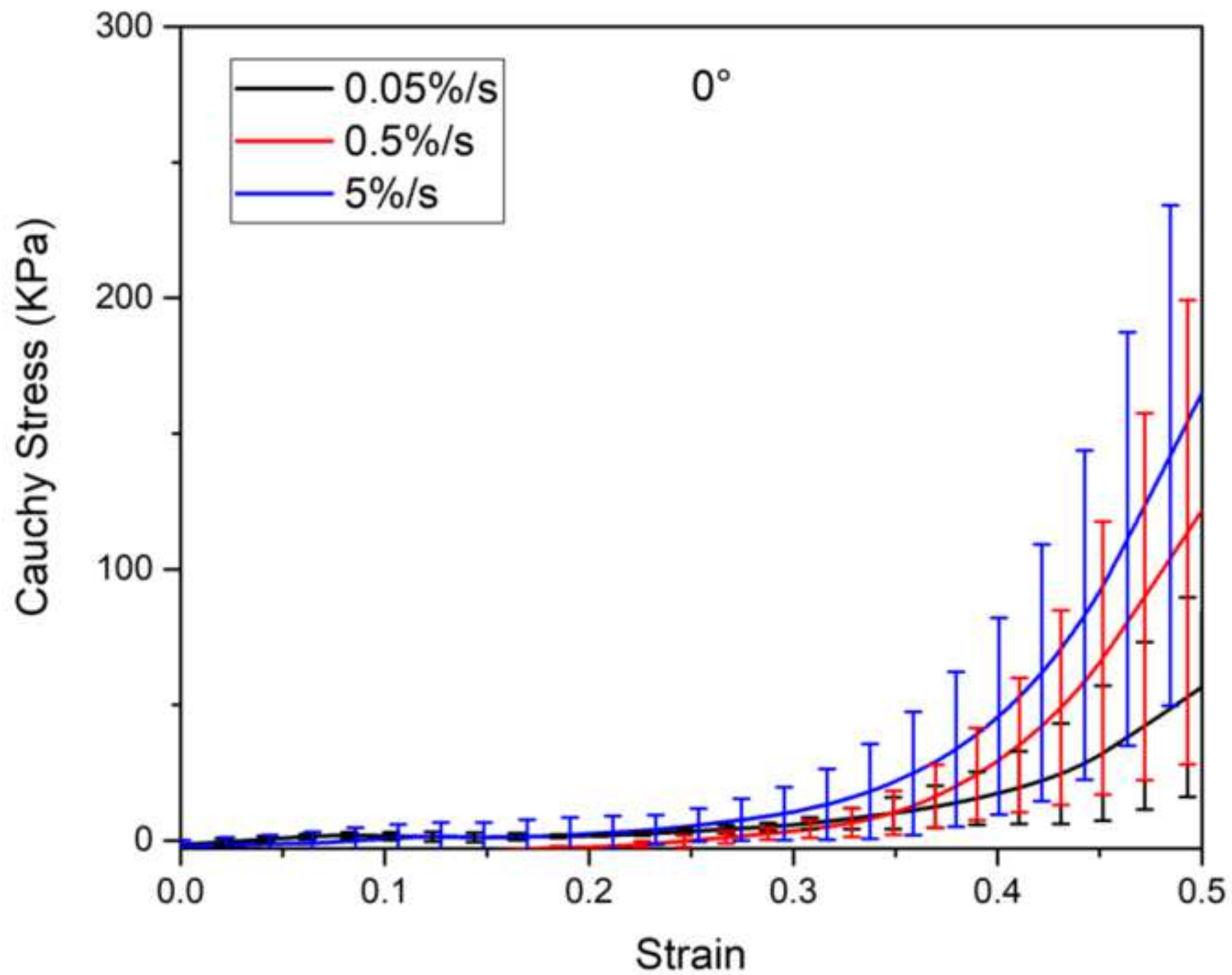
$90^\circ$

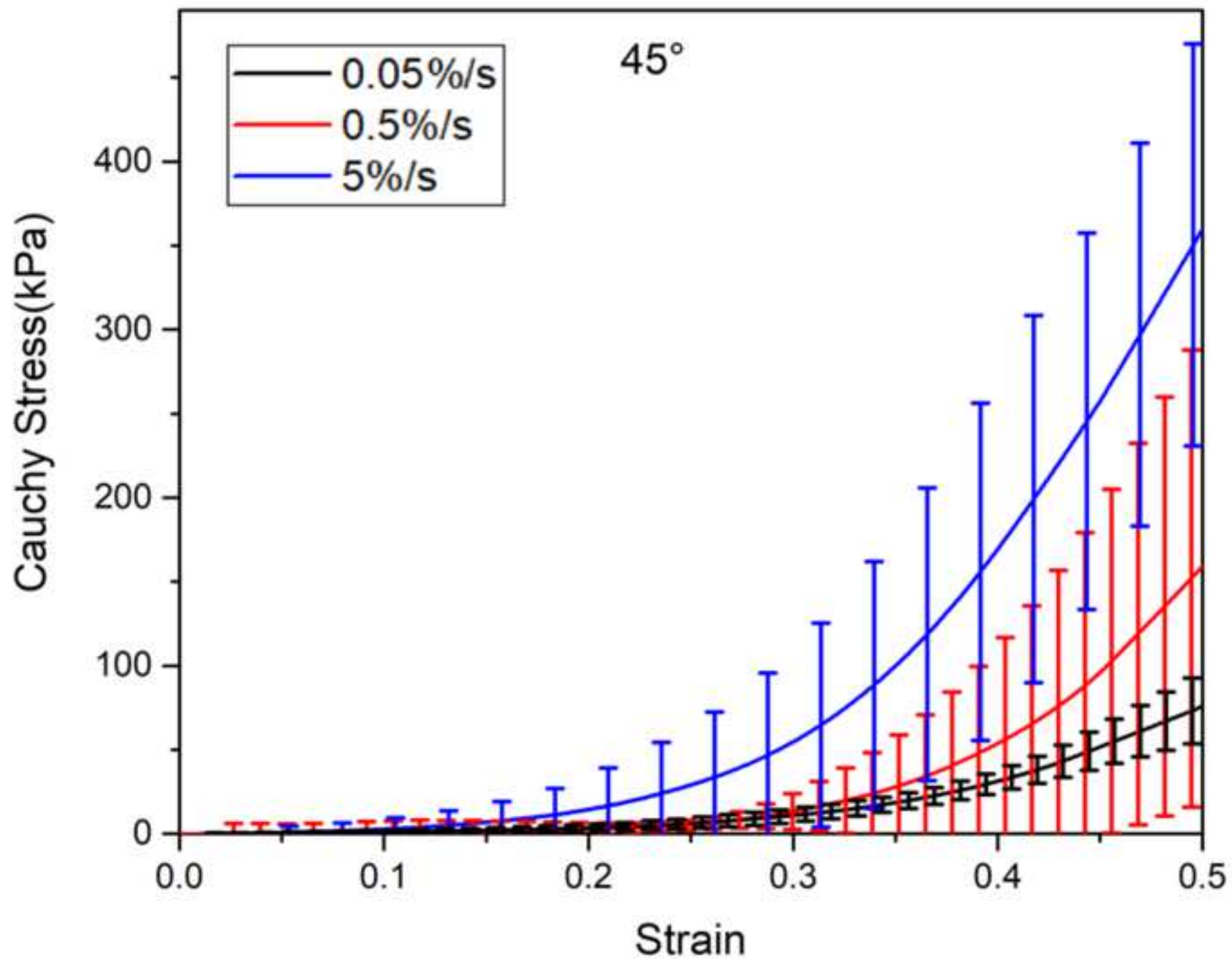


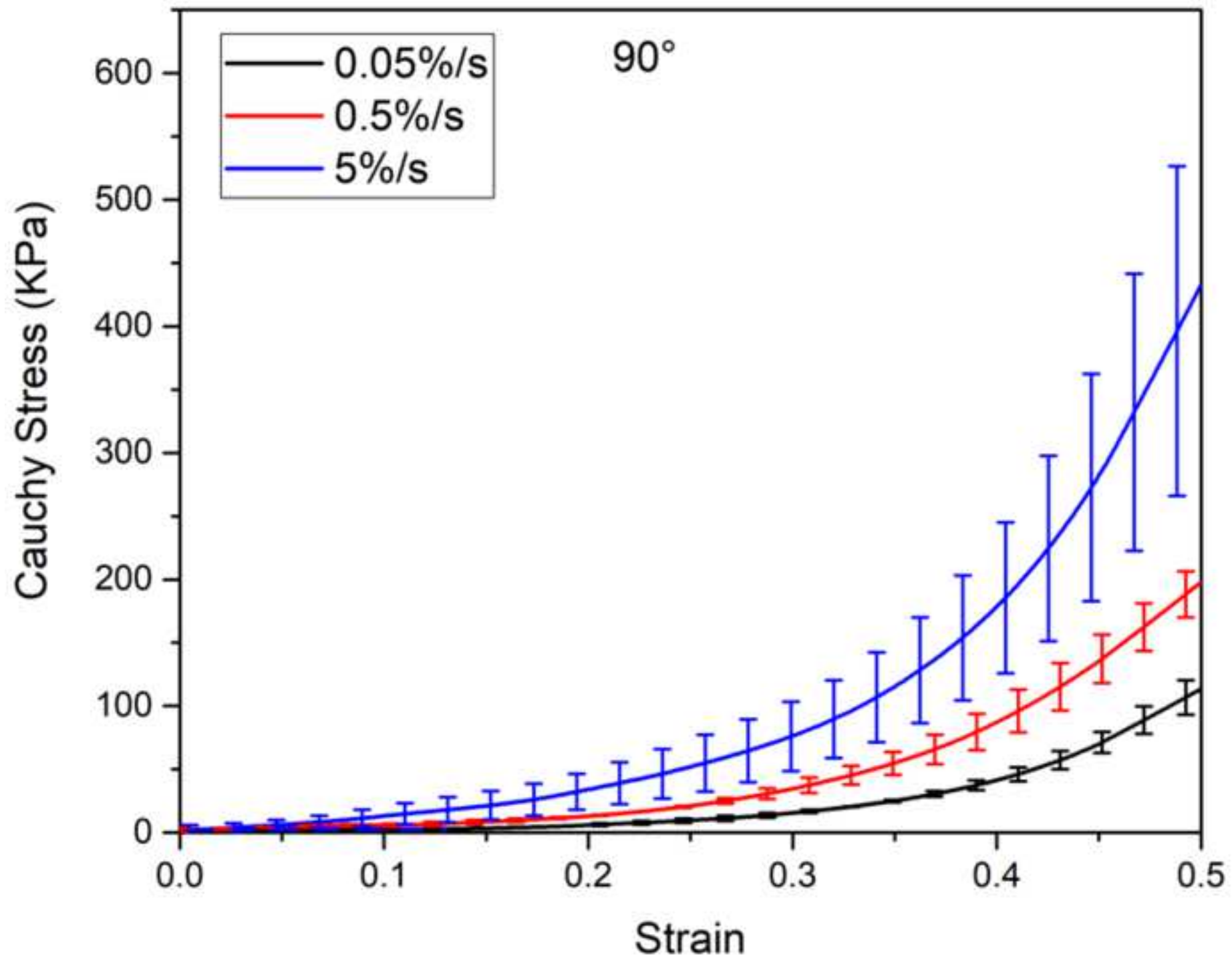


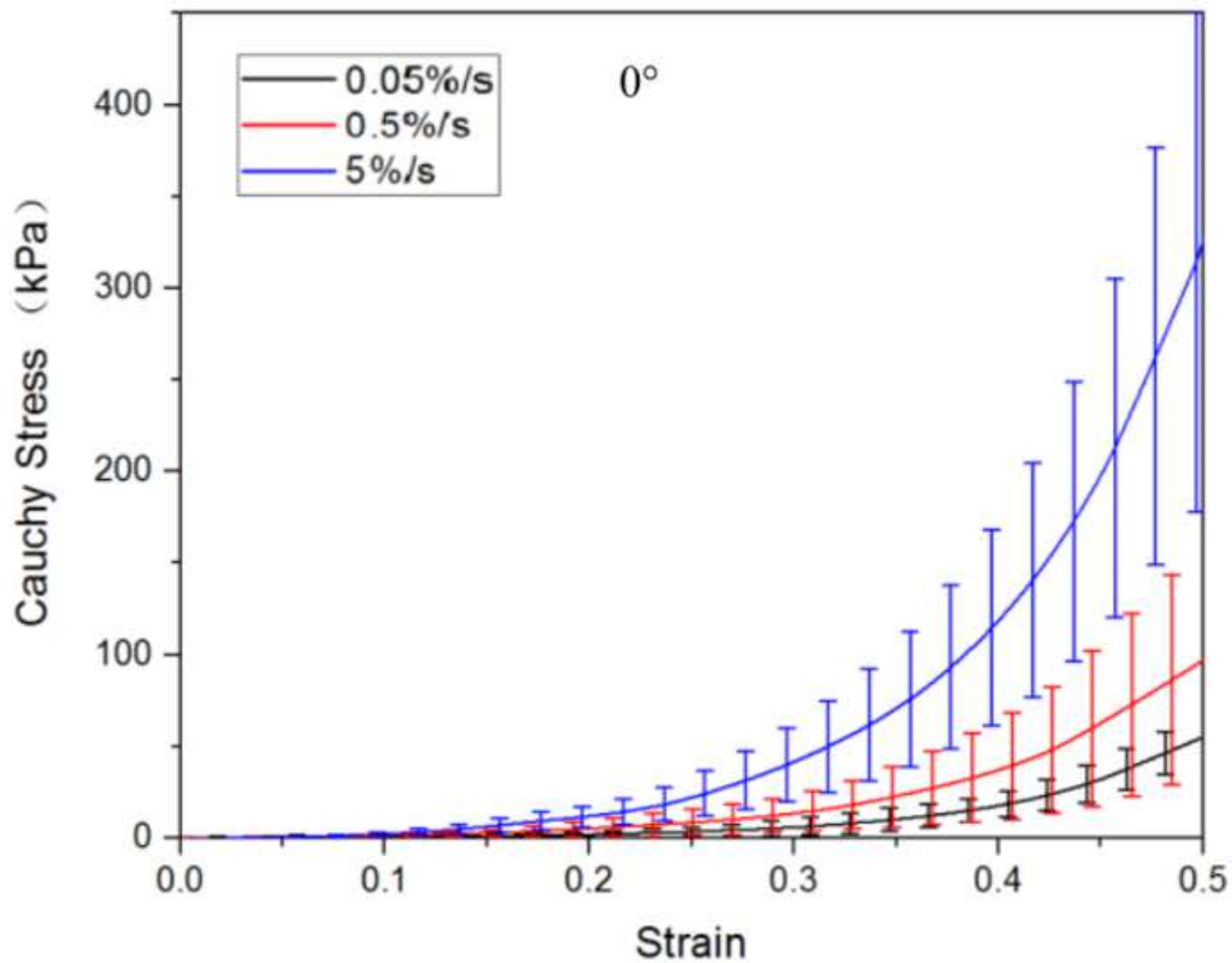


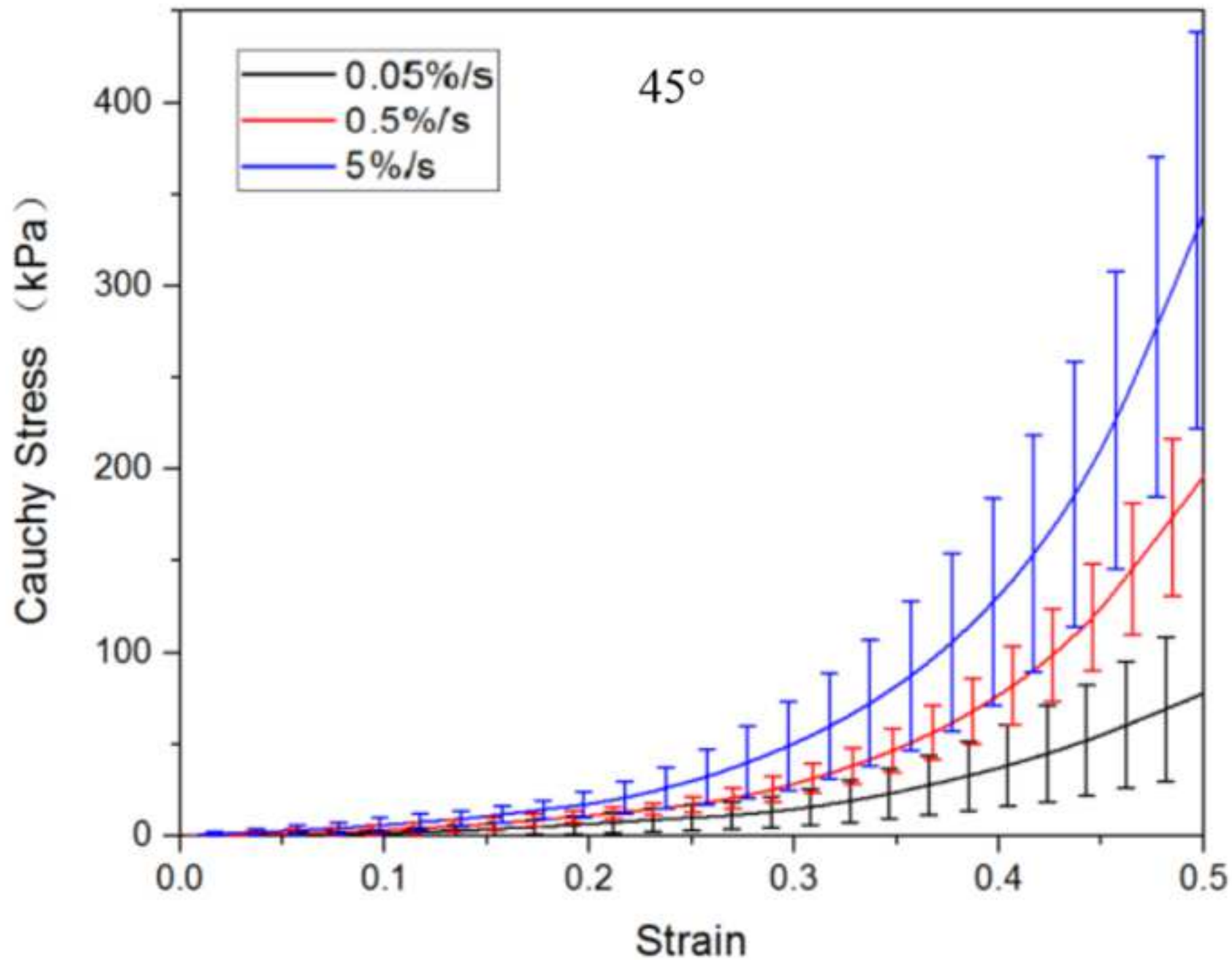


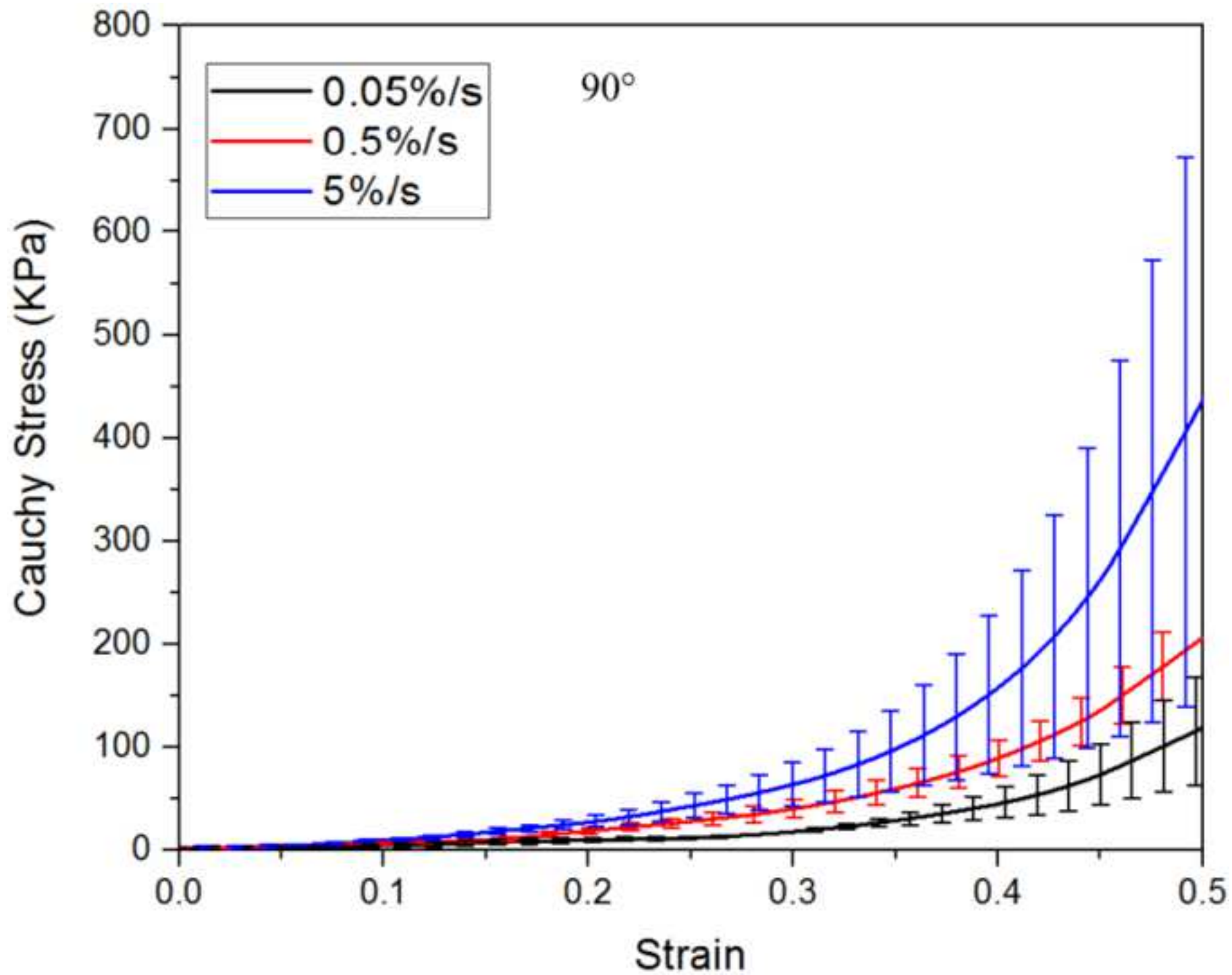


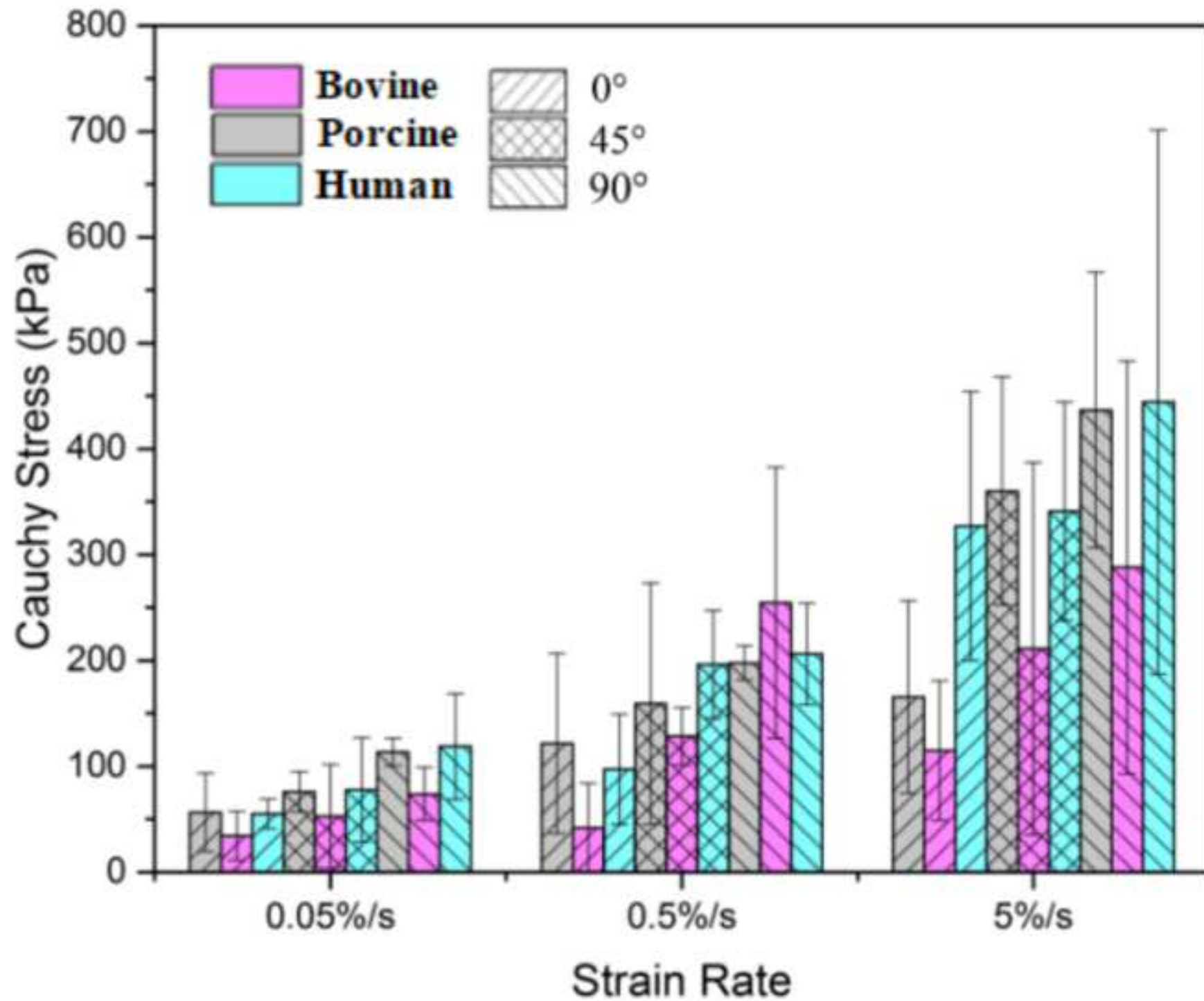


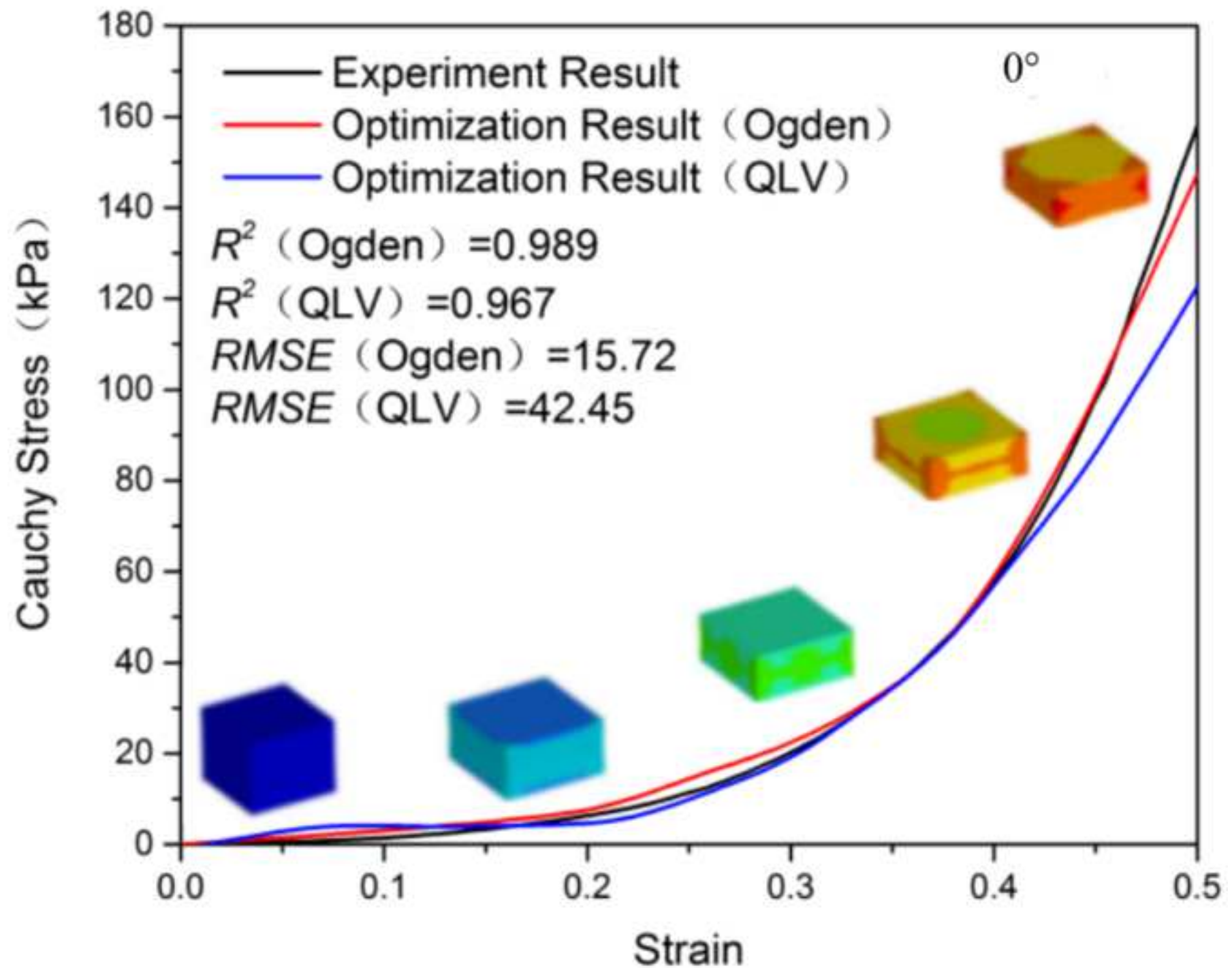


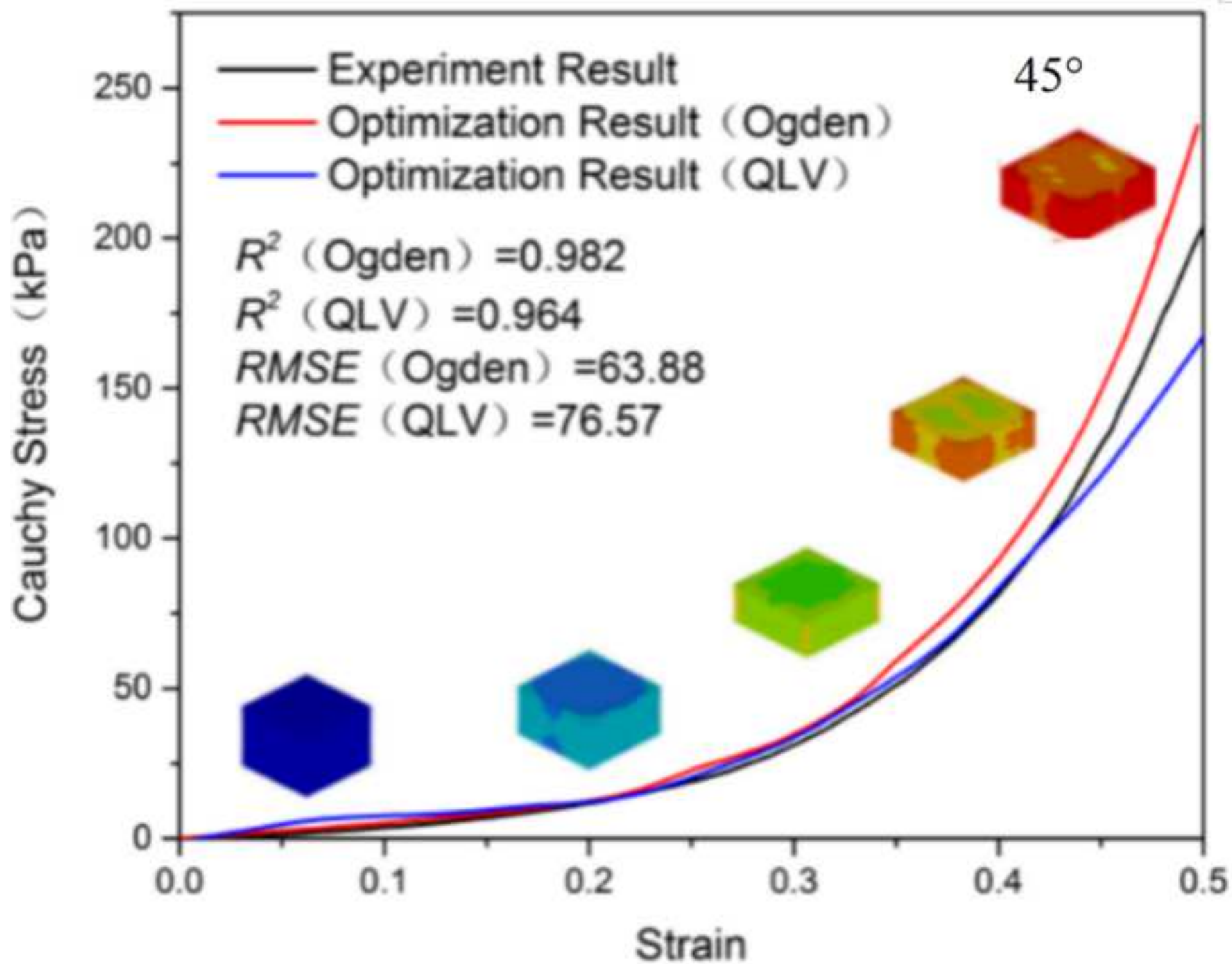


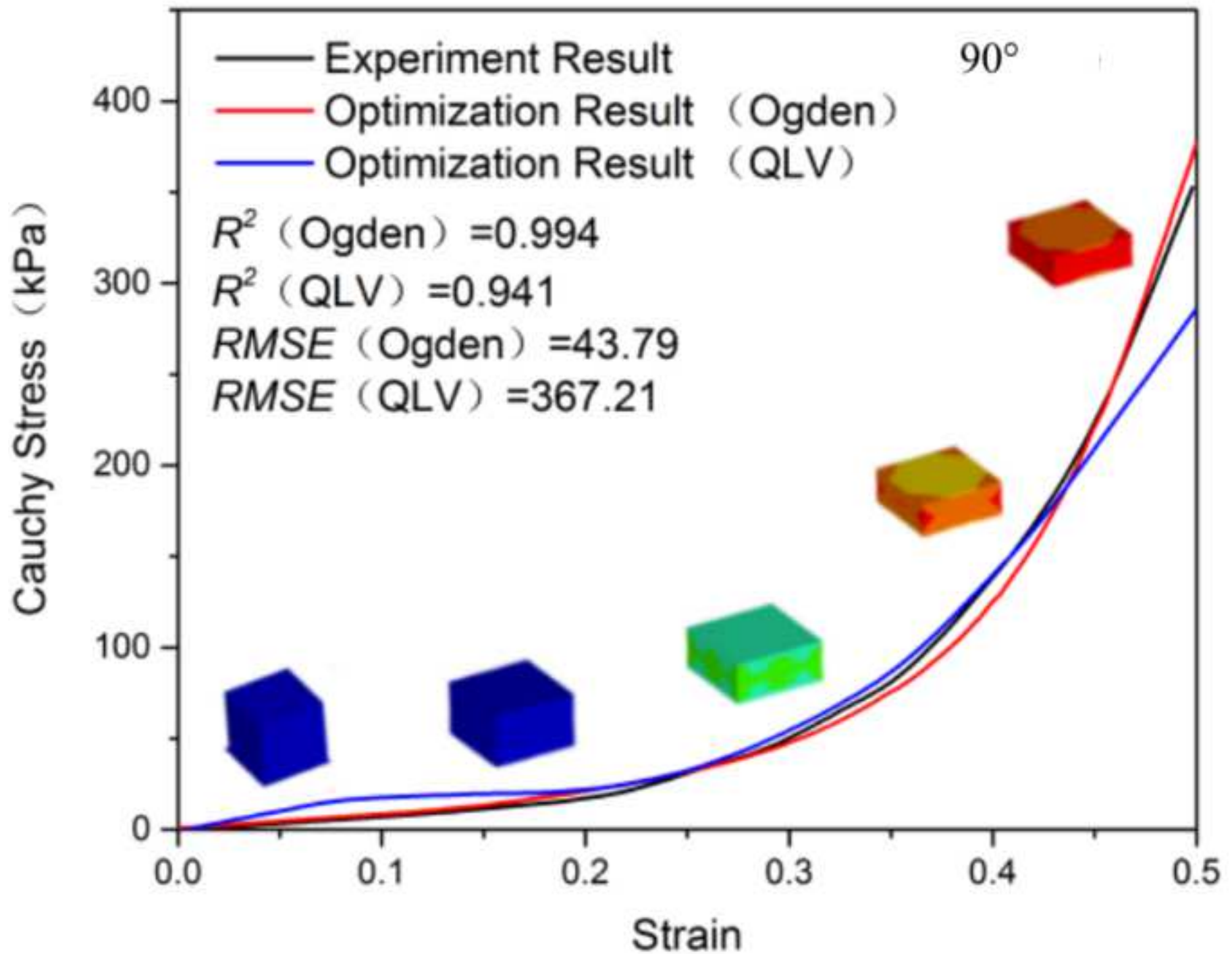












## **Conflict of Interest Statement**

Fuhao MO, Zhefen ZHENG, Haotian ZHANG, Guibing LI, Zurong YANG, Deyi Sun, J Biomechanics

**Title:** In vitro compressive properties of skeletal muscles and inverse finite element analysis: comparison of human versus animals

The authors assert that there are no conflicts of interest of any type.  
This assertion is also included in the manuscript.

**Fuhao MO:** Conceptualization, Methodology, Writing- Reviewing and Editing, Supervision;

**Zhefeng ZHENG:** Data curation, Formal analysis, Writing- Original draft preparation;

**Haotian ZHANG,** Software, Validation;

**Guibing Li:** Investigation, Visualization;

**ZuRong YANG:** Validation;

**Deyi Sun:** Resources, Writing- Reviewing and Editing, Supervision.